crystals

MDPI

Article

Electron Beam Welding of Copper and Aluminum Alloy with Magnetron Sputtered Titanium Filler

Darina Kaisheva [1,2,*], Georgi Kotlarski [1], Maria Ormanova [1], Angel Anchev [3], Vladimir Dunchev [3], Borislav Stoyanov [4] and Stefan Valkov [1,5]

1 Academician Emil Djakov Institute of Electronics, Bulgarian Academy of Sciences, 72 Tzarigradsko Chausse Blvd, 1784 Sofia, Bulgaria; gvkotlarski@gmail.com (G.K.); m.ormanova@ie.bas.bg (M.O.); stsvalkov@gmail.com (S.V.)
2 Department of Physics, Neofit Rilski South-West University, 66 Ivan Michailov Str., 2700 Blagoevgrad, Bulgaria
3 Department of Material Science and Mechanics of Materials, Technical University of Gabrovo, 4 H. Dimitar Str., 5300 Gabrovo, Bulgaria; anchev@tugab.bg (A.A.); v.dunchev@tugab.bg (V.D.)
4 Department of Industrial Design and Textile Engineering, Technical University of Gabrovo, 4 H. Dimitar Str., 5300 Gabrovo, Bulgaria; stoyanov_b@mail.bg
5 Department of Mathematics, Informatics and Natural Sciences, Technical University of Gabrovo, 4 H. Dimitar Str., 5300 Gabrovo, Bulgaria
* Correspondence: darinakaisheva@abv.bg

Abstract: In this work, the results from the electron beam welding of copper and Al6082T6 aluminum alloy with a titanium filler are presented. The influence of the filler on the structure and mechanical properties of the welded joint is studied in comparison with one without filler. The X-ray diffraction (XRD) method was used to obtain the phase composition of the welded joints. Scanning electron microscopy (SEM) was used for the study of the microstructure of the welds. Energy-dispersive X-ray spectroscopy (EDX) was applied to investigate the chemical composition. The mechanical properties were studied by means of microhardness measurements and tensile tests. A three-phase structure was obtained in the fusion zone consisting of an aluminum matrix, an intermetallic compound $CuAl_2$, and pure copper. The application of Ti filler significantly decreased the amount of molten copper introduced in the molten pool and the number of intermetallic compounds (IMCs). This improved the strength of the joint; however, some quantity of IMCs was still present in the zone of fusion (FZ), which reflected the microhardness of the samples. The application of a titanium filler resulted in refining the electron beam weld's structure. The finer structure and the reduced amount of the brittle intermetallic phases has led to an increase in the strength of the joint.

Keywords: electron beam welding; dissimilar metals; aluminum; copper; titanium filler; DC magnetron sputtering

check for updates

Citation: Kaisheva, D.; Kotlarski, G.; Ormanova, M.; Anchev, A.; Dunchev, V.; Stoyanov, B.; Valkov, S. Electron Beam Welding of Copper and Aluminum Alloy with Magnetron Sputtered Titanium Filler. *Crystals* **2024**, *14*, 752. https://doi.org/10.3390/cryst14090752

Academic Editor: Liqun Li

Received: 19 July 2024
Revised: 16 August 2024
Accepted: 23 August 2024
Published: 24 August 2024

Copyright: © 2024 by the authors. Licensee MDPI, Basel, Switzerland. This article is an open access article distributed under the terms and conditions of the Creative Commons Attribution (CC BY) license (https://creativecommons.org/licenses/by/4.0/).

1. Introduction

One of the oldest and, at the same time, most widely used methods for creating a joint between two metals is welding. In the past, production was limited to welding metals of the same kind. Nowadays, in response to the growing needs of various industries, the welding of dissimilar metals is increasingly required [1–3]. This process is a challenge for engineers and technicians due to the different chemical compositions and different thermophysical properties of the two dissimilar metals or alloys, especially in fusion technologies. The factors that affect the quality of the welds in fusion welding are physical, such as the boiling and melting temperatures of the materials, specific thermal conductivity, specific heat capacity, and coefficient of thermal expansion, and chemical ones, such as the ability to form solid solutions, chemical compounds, and eutectics, crystal lattice and structure, wettability of one metal to other, and solubility limitations [4].

Despite the difficulties in fusion welding technologies mentioned above, electron beam welding (EBW) has a higher number of advantages than other welding technologies [5]. The main advantage is the high energy density and efficient energy conversion. The process takes place in a vacuum, and therefore, no oxidation occurs; moreover, no additional materials are required, and this ensures a weld seam without impurities. As a result of the rapid execution of the process, a seam with an extremely high depth-to-width ratio (h/b up to 40:1) is obtained with a narrow heat-affected zone. Last but not least, the process is repeatable and can be precisely controlled by changing the technological conditions.

Copper and aluminum are metals that are widely used in automobile, ship, and aircraft construction, as well as in the electrical industry and electronics [6–8]. These metals have excellent electrical and thermal conductivity and very good corrosion resistance, and aluminum also has a very low density [9,10]. Their use, on the one hand, leads to obtaining a compound with desirable properties, combining the advantages of each of the two metals, and on the other hand, it leads to a reduction in costs when replacing traditional materials, such as steel, with them. Aluminum is cheaper and lighter than copper, so if copper is partially replaced by aluminum in a component, it will reduce the cost of both production and use due to energy savings.

A problem when welding a copper/copper alloy with an aluminum/aluminum alloy is the formation of brittle intermetallic compounds (IMCs) that reduce the mechanical properties of the joint [3,11,12]. Different technologies have been applied to decrease the number of IMCs [13–15]. Solid-state welding technologies, mainly friction stir welding, are commonly used for Cu/Al joining [16–18]. In friction welding, ultrasonic welding, and magnetic pulse welding [3,19,20], there is low heat input, and this leads to the formation of thin IMC layers. It is known that the highest solid solubility of copper in aluminum is 5.8% at 548 °C. At room temperature, the copper in a Cu/Al interface is present in the form of a combination of a saturated solid solution and dispersed in the structure as part of fine precipitates of the $CuAl_2$ phase [21]. Due to the mechanisms of welding using friction stir welding, the possibility of forming a weld seam with accurate dissolution of Cu in the Al alloy can be achieved relatively easily by optimizing the technological conditions of welding. However, applying additional pressure when joining the materials can compromise the grain structure and cause irregularities in the base material. Additionally, solid-state welding techniques have limitations in automated control, repeatability, and flexibility. In fusion technologies, such as laser and electron beam welding, a powerful heat source melts the metals, and metallurgical reactions take place. A few ways to decrease the number of intermetallic phases in laser beam welding of Cu/Al have been reported in a number of articles [22,23]. The research shows that it is not possible to completely avoid the formation of intermetallics.

Factors affecting the formation of intermetallic compounds when welding dissimilar materials are dilution between the base metals, physical properties, welding parameters, filler metal, and heat treatment [11]. In order to reduce the influence of different thermo-physical parameters and the poor metallurgical compatibility of copper and aluminum, as a result of which intermetallic compounds are formed, it is necessary to take the following actions: control the temperature and duration of the molten pool, control the ratio between the molten quantities of both metals, reduce the amount of copper melted, and control the homogenization of the melt. All of these actions can be performed by choosing appropriate technological conditions. Technological conditions include the electron beam power, the welding speed, the scan geometry of the beam, etc., as well as the application of suitable fillers in the welding gap.

In previous studies [24,25], the effect of the technological conditions of EBW on the structure and mechanical properties of Cu/Al joints was investigated. The conclusion that a circular beam oscillation with a radius of 0.2 mm leads to a decrease in the number of IMCs was made. It was also concluded that this led to a refining of the grain structure of the formed welds.

As was mentioned, the application of an appropriate filler can reduce the formation of intermetallic compounds. Both pure metals and metal alloys can be used as fillers [7]. The authors of [26] report their results on using different filler wires during the process of pulsed double electrode gas metal arc welding (DE-GMAW). They used four different fillers in the form of wires, namely, the aluminum alloys ER1100 (Al99.5), ER5356 (AlMg5Cr), ER4043 (AlSi5), and ER4047 (AlSi12). Their study concluded that with the increase in the Si content in the case of Al–Si filler wires, the thickness of the intermetallic compound layers decreased noticeably. The authors of [27] show the effect of two different fillers—Ag and Ni—in the form of a foil on IMC formation in laser micro-welding of pure Cu and pure Al. According to them, the use of silver foil leads to a significant improvement in the tensile strength and the dynamic fatigue behavior of the welded samples. The effect of Al content in Zn–Al filler in the laser brazing of a Cu/Al joint is investigated in [28]. Up to this point, however, very limited knowledge on the application of appropriate filler material is present regarding the electron beam welding of copper and Al and their alloys.

Titanium is a highly prospective material that can be used as a filler material. Conventional techniques, such as magnetron sputtering, have already been used for decades for the formation of pure Ti and Ti-based coatings. Furthermore, Ti has relatively good electrical and thermal conductivities; however, they are much lower than those of Cu and Al. In addition, Ti has a higher melting temperature than both Cu and Al, but it is still somewhat close to that of copper. This means that melting Ti during the electron beam welding process should not be a substantial issue, theoretically. Possible other fillers that can be used during the electron beam welding of Cu and Al are Mo and V; however, their melting temperatures are too high for their successful introduction in the melt pool in a liquidus state.

Due to this, the main goal of this research is the investigation of the effect of applying Ti as a filler material in the welding gap during the EBW of pure copper and an aluminum alloy, specifically, Al6082T6. The Ti filler was deposited using a DC magnetron sputtering on the welding plates. The structure of the weld seams obtained with and without a filler was examined. New insight was brought into the resultant functional properties of the studied samples as a function of the technological conditions.

2. Materials and Methods

Pure copper (Cu) and an Al6082T6 aluminum alloy were used in the experiments. Welding plates with dimensions of 100 × 50 × 8 mm were used. A thin film of Ti was deposited on the cross-sections of the plates with dimensions of 100 × 8 mm. Prior to the deposition stage, the process of cathodic cleaning was performed using the following technological conditions: Ar gas pressure of 8×10^{-2} mbar, plasma potential of 900 V, and plasma current of 0.1 A, for 10 min. Second to this process, the filler layers were deposited at a working pressure of 1×10^{-3} mbar. The power of the discharge process was 440 W, with the current being set to 1 A. The Ti film was sputtered for 180 min. The thicknesses of the coatings are in the range of 9–10 μm, depending on the studied sample. The large variation of the thickness is caused by the large area of deposition, which causes irregularities in the coatings' growth rates. The process of the deposition of the filler layers is schematically represented in Figure 1.

After the filler film was deposited on the contact surfaces of the copper and aluminum alloy plates, the electron beam welding process was implemented. An Evobeam Cube 400 (Evobeam GmbH, Nieder-Olm, Germany) welding unit was used to carry out the EBW. The schematic of the welding process of the Cu and Al6082T6 plates with the Ti filler is shown in Figure 2. The technological conditions were as follows: welding speed v = 15 mm/s; accelerating voltage U = 60 kV; and beam current I_b = 45 mA. The electron beam was deflected toward the aluminum alloy plate at a distance of d = 0.5 mm. A circular oscillation of the beam with a radius of 0.2 mm was applied. Preliminary experiments were performed using a beam offset toward the aluminum plate of 0.2 mm, 0.3 mm, and 0.4 mm. In addition, the same experiments were carried out without circular oscillations and with

an oscillation of 0.1 mm. The resulting weld seams were either too shallow or with too high a concentration of defects. Due to this, both the circular oscillation radius and the beam offset were increased to the values selected in this work. Prior to the welding process, the plates were preheated to a temperature of 200 °C. The technological conditions applied in this work are based on the collective knowledge and prior experience of the researchers involved in this work [24,25,29].

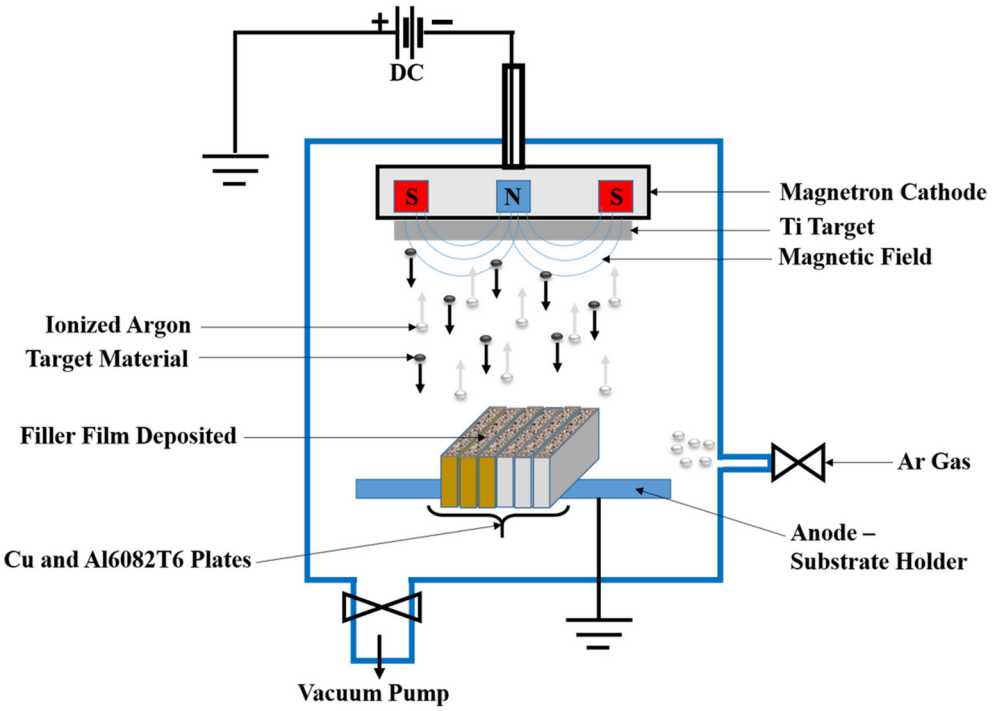


Figure 1. Scheme of the direct current magnetron sputtering process.

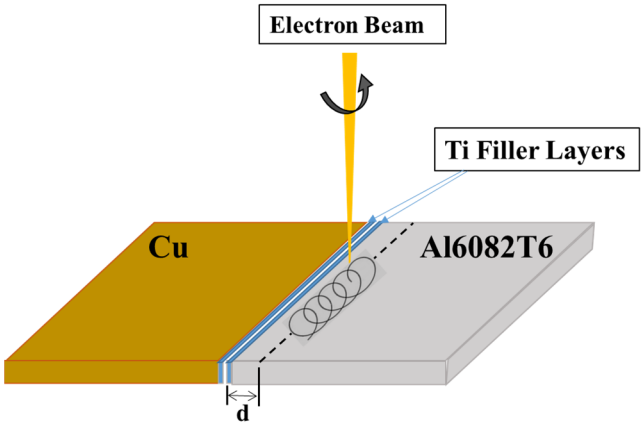


Figure 2. Scheme of the EBW of Cu and Al6082T6 with titanium filler.

The obtained samples were studied by means of a phase analysis, scanning electron microscopy, and mechanical tests. The phase analysis was performed using an X-ray diffractometer "Bruker D8 Advance" (Brucker Corp., Billerica, MA, USA). CuKα characteristic radiation with a wavelength of 1.54 Å was used. The measurements were performed in the range of 25 to 85 degrees, with a step of 0.1 degrees, and a registration time of 0.5 s per step was applied. All detected phases were identified using the following International Centre for Diffraction Data (ICDD) database power diffraction files (PDFs: #040787, #040836, #441294, and #250012.

The structure of the welded specimens was investigated via scanning electron microscope (SEM) "LYRA3 I XMU" (TESCAN ORSAY HOLDING, a.s., Kohoutovice, Czech Republic). Back-scattered electrons were employed. The chemical elements' distribution in the welds was determined using an energy-dispersive X-ray spectroscope (EDX) "Quantax 200" (Brucker Corp., Billerica, MA, USA).

A ZwickRoell Dura Scan 10/20 G5 (ZwickRoell, Ulm, Germany) semi-automatic microhardness tester was used for the Vickers hardness measurement. A load of 50 g (load force of 0.5 N) was applied. The measurements were performed following a linear trajectory perpendicular to the weld at a depth of 1 mm below the surface of the samples. The experiments were performed according to the ISO 6507-1 standard [30].

A ZwickRoell Vibrophore 100 (ZwickRoell, Ulm, Germany) tensile tester at static mode was used for the tensile experiments. A constant stress rate of 30 MPa/s was applied. The measurements were conducted in accordance with the ISO 6892-1-Method B standard [31]. For the purpose of this experiment, three tensile test samples were produced for each of the used technological conditions of electron beam welding. The samples had a total length of 92 mm, a length of the test area of 40 mm, a width of the test area of 13 mm, and a thickness of 8 mm. A graphical representation of the tensile test samples and a detailed schematic of the dimensions of the latter were included in a previous work [32].

3. Results

Figure 3 shows the results of the X-ray diffraction experiments performed on both samples. Figure 3a shows the results obtained for the sample prepared without any filler materials, and Figure 3b shows the results obtained for the sample prepared using Ti filler. All obtained diffraction patterns do not exhibit the presence of amorphous-like halos, which confirms that during the welding process, the entire volume of the weld seam successfully recrystallized and formed its characteristic polycrystalline structure. During the experiments, copper and aluminum phases were detected in their typical face-centered cubic (fcc) crystal lattice structure. A titanium phase with a hexagonal closed-packed (hcp) crystal structure was also observed in the case of the sample in which the Ti filler was used during the welding process. In both cases, intermetallic phases were also detected, in particular, the $CuAl_2$ phase, which has a tetragonal crystal structure [33]. Comparatively, it is estimated that a much higher intensity of $CuAl_2$ diffraction maxima is observed in the case of the first sample. Also, in the case of the second sample, only a single diffraction peak of the Cu phase was detected. This suggests two things. Firstly, the application of the Ti filler and the employment of a beam offset toward the aluminum plate limited the applied heat to the copper plate. This, in turn, limited the quantity of the molten Cu phase, which was introduced in the welded joint. As mentioned above, even small quantities of copper in the aluminum solid solution are enough to oversaturate it, beyond which point an uncontrollable formation of IMCs occurs. It is possible that the application of the Ti filler limited the concentration of copper in the weld pool, thus also limiting the formation of IMCs.

In Figure 4, different magnification SEM images are presented of the cross-section of the weld seam of the Cu/Al6082T6 joint without the filler. The cross-section of the formed butt joint, as shown in Figure 4b, suggests that the full penetration of the weld beam in the structure of the plates was achieved. The standard for EBW "keyhole" shaped weld seam has formed, with most of its contents seemingly being composed of aluminum. Figure 4a shows a zoomed image of the border between the fusion zone (FZ) and the copper plate. Figure 4d shows an even more zoomed image of the same area, consisting of an unevenly mixed compound. In order to further investigate and differentiate them an EDX analysis was performed, and the results are summarized in Table 1. The points marked as "1" and "2" in the image were studied. The results showed that in the case of the first point, a predominantly copper content was found. In the case of the second point, a 65%/35% mixture of aluminum and copper was reported. This suggests that the point either contains formations of IMCs or a mixture of an αAl solid solution with IMC incisions of the type αAl

+ IMCs. Figure 4c depicts an image of the boundary between the zone of fusion (FZ) and the aluminum plate. Figure 4f depicts a zoomed image of that area. Much more pronounced agglomerates are visible in this case. Once again, an EDX analysis was performed, and the composition of points "5" and "6" was studied. Apparently, the visible agglomerates have a 70%/30% Al/Cu composition, which corresponds to the $CuAl_2$ phase. In the case of point "6" an almost pure aluminum composition was detected. Finally, a zoomed image of the center of the weld seam is given in Figure 4e. Large agglomerates are visible in this case, with a seemingly larger density compared to those closer to the aluminum plate. Once again, their composition was studied using EDX, and it was confirmed that those agglomerates (point "3") have the same composition as the ones shown in Figure 4f, namely, a 70%/30% mixture of Al/Cu. Point "4" exhibited an almost pure aluminum content. This suggests that most probably, the agglomerates observed in the case of this sample, both in the center of the weld seam and along its edges, belong to the $CuAl_2$ intermetallic phase. These results are confirmed by the previous investigations of Cai et al. [34], who have studied the microstructure and properties of cold metal transfer welded joints of Cu and Al.

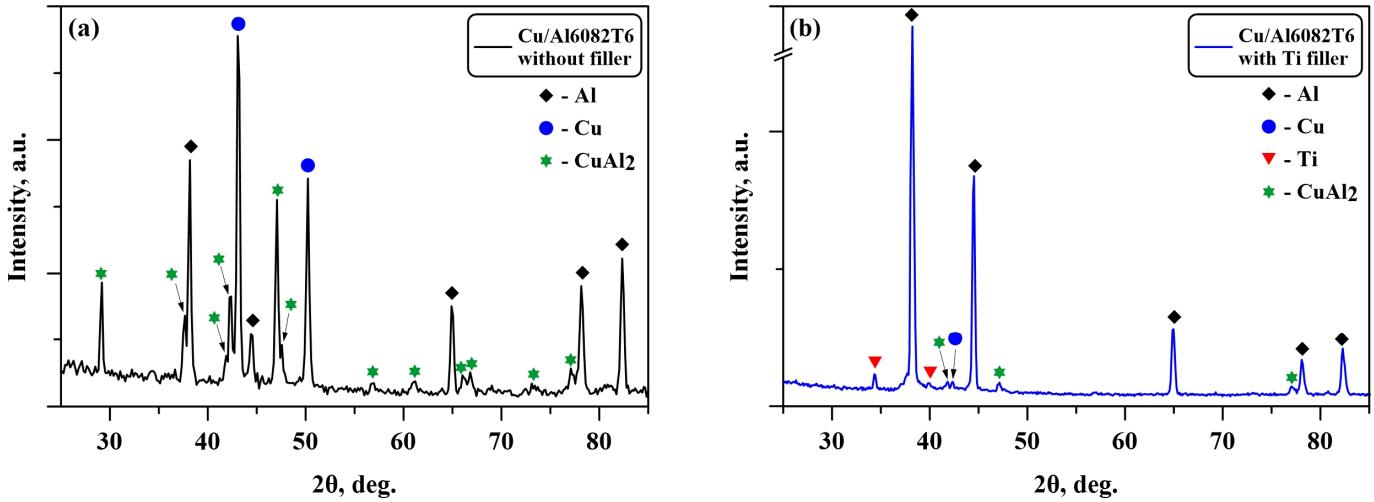


Figure 3. X-ray diffraction patterns of the welded Cu/Al6082T6 joints (**a**) without filler and (**b**) with Ti filler.

Figure 5 presents SEM images of the cross-section of the sample formed using a Ti filler. Figure 5b shows a macro image of the formed weld seam. Similar to the previous sample, in this case, full penetration of the electron beam was achieved. The chemical composition of the formed welded joint was studied using energy-dispersive X-ray spectroscopy, and the results are presented in Table 2. Figure 5a depicts the border between the copper plate and the fusion zone, and Figure 5d depicts a zoomed image of the studied area. EDX analysis was performed in the points marked as "1", "2", and "3". The results indicate that most of the composition of point "1" is composed of copper. In the case of points "2" and "3", the results indicated a 13%/87% and 37%/63% ratio between the copper and the aluminum content, respectively. The 13%/87% ratio most probably corresponds to a mixture of an aluminum solid solution and IMCs of the type αAl + IMCs. The other ratio of 37%/63% most probably corresponds to the $CuAl_2$ phase. As discussed above, the observed agglomerates are believed to be inclusions of the $CuAl_2$ intermetallic phase spread across the volume of the weld seam. Figure 5c depicts the boundary between the aluminum plate and the fusion zone. The EDX analysis performed in the zoomed section of that area, as depicted in Figure 5f, indicates that point "7" has over 99% concentration of Al, and point "6" has a 26%/73% ratio between copper and aluminum. Figure 5e depicts a zoomed section of the middle of the weld seam. An EDX analysis was performed in this area, as well. A darker section marked as point "5" was studied, and the results show that this area is mostly composed of aluminum. The studied in point "4" agglomerates

have a composition of 51%/49% Cu/Al. This result is interesting and possible for one of two reasons. Either this corresponds to the CuAl intermetallic phase or, due to limitations of the analytical method, a higher concentration of copper was detected, belonging to a close proximity agglomerate. Since no other agglomerates are visible close to the studied area, it is most likely that this result indicates the presence of the CuAl phase. Evidently, despite its presence in the volume of the weld seam, its concentration is not high enough to be detected by the diffractometer. This IMC, along with others, was also detected by Fu et al. [35]. In all studied areas, small concentrations of the Ti phase were detected, with an average concentration of 0.26 at.%.

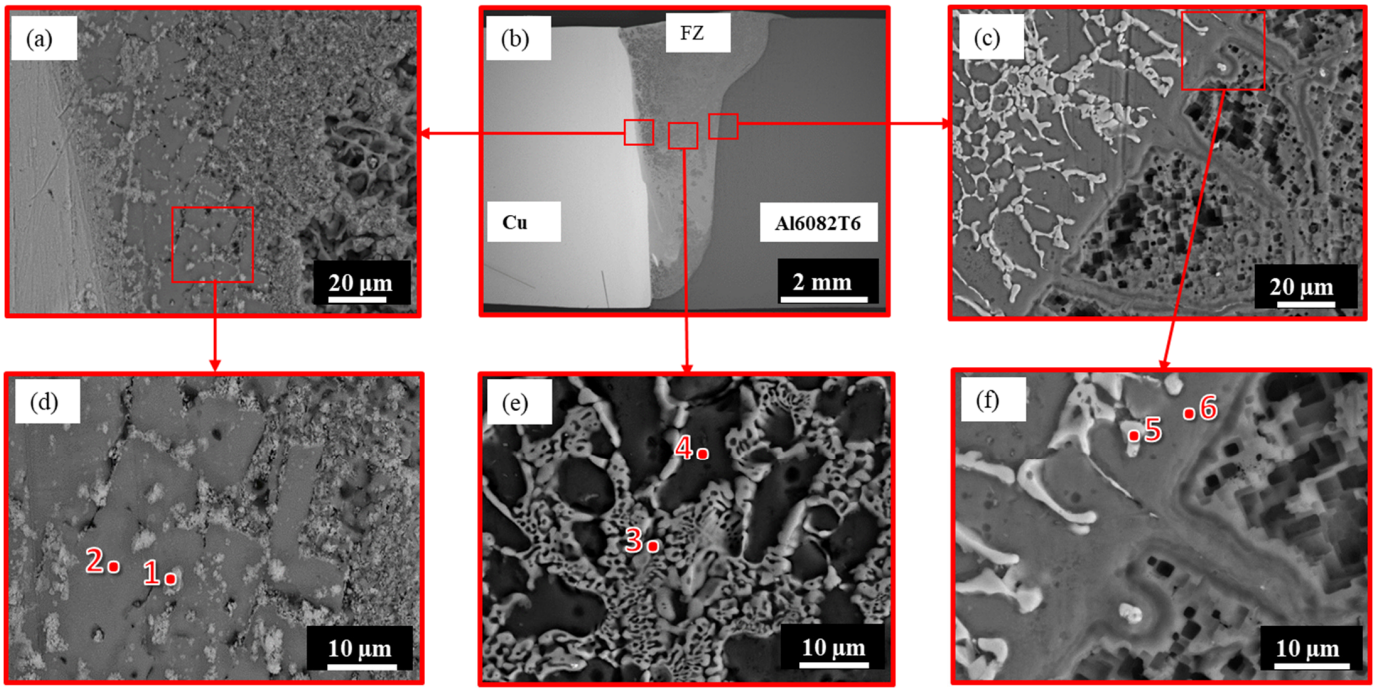


Figure 4. SEM images of the cross-section of the Cu/Al6082T6 specimen without filler: (**a**) interface between the copper plate and the zone of fusion; (**b**) whole weld seam; (**c**) FZ-Al6082T6 interface; (**d**) image of the Cu-FZ interface; (**e**) image of the FZ; (**f**) image of the border between the zone of fusion and the Al6082T6 plate.

Table 1. Chemical compounds comprising the formed joint without filler.

Element	Cu, at.%	Al, at.%	Possible Phase
Point 1	84.41 ± 2.7	15.59 ± 0.5	Cu
Point 2	35.72 ± 1.7	64.28 ± 2.1	$CuAl_2$
Point 3	30.95 ± 1.8	69.05 ± 2.6	$CuAl_2$
Point 4	1.97 ± 0.4	98.03 ± 5.3	Al
Point 5	30.49 ± 1.6	69.51 ± 2.4	$CuAl_2$
Point 6	1.44 ± 0.3	98.56 ± 5.4	Al

The measured microhardness is given in Figure 6. Figure 6a depicts the results for the sample formed without using a filler. The microhardness of the aluminum plate is about 60 $HV_{0.05}$, and the microhardness of the copper plate is about 50 $HV_{0.05}$. Entering the fusion zone, the microhardness values rapidly spike and reach maximum values of 210 $HV_{0.05}$. Large fluctuations of the values are observed, with the lowest detected value being 128 $HV_{0.05}$. The large fluctuations suggest that the structure of the weld seam is highly non-homogeneous. Figure 6b shows the results of the microhardness measurements of the sample produced with the Ti filler. The microhardness of the plates is about the same as in the previous sample and is typical for these kinds of materials [36,37]. However, a

noticeable difference is present in the microhardness of the fusion zone. A smooth increase in the microhardness from the Cu plate toward the FZ is observed, followed by a smooth decrease going toward the Al plate. The maximum microhardness measured in the fusion zone was 235 $HV_{0.05}$, and the lowest was 165 $HV_{0.05}$. Proportionally, the first sample exhibited a microhardness difference from the maximum to the minimal value of 82 $HV_{0.05}$, and the Ti filler sample exhibited a value of 70 $HV_{0.05}$. Evidently, the difference is not too high; however, the Ti filler sample does indeed exhibit a slightly better unification of the measured values. For this reason, it can be concluded that the structure of the Ti filler sample is slightly more homogeneous. Regarding the microhardness values themselves, a study of the microhardness in the interface between Cu and Al composites was carried out by the authors of [38], who have found a direct correlation between the cooling rate and the resultant microhardness. They reported that an increase in the cooling rate leads to an increase in the microhardness [38]. This trend is also true regarding the results of this work since electron beam welding is characterized by a high cooling rate [39]. Due to this, the resultant hardness in the fusion zone has high values. In addition, the introduction of the Ti filler in the second sample results in a smooth increase in the microhardness since the highest cooling rate is observed in the middle of the weld seam. The Ti filler apparently sufficed to modulate the cooling rate by slowing it down closer to the base materials. This is confirmed by both the SEM and XRD analyses. It is also important to mention that the microhardness of the Al6082T6 alloy, as mentioned above, is theoretically supposed to be much higher. This microhardness is achieved by means of a heat treatment process; however, previous studies have proven that applying heat above 300 °C to heat-treated aluminum alloys reverses the process of heat treatment, and the alloy once again exhibits its original structural and mechanical properties [40].

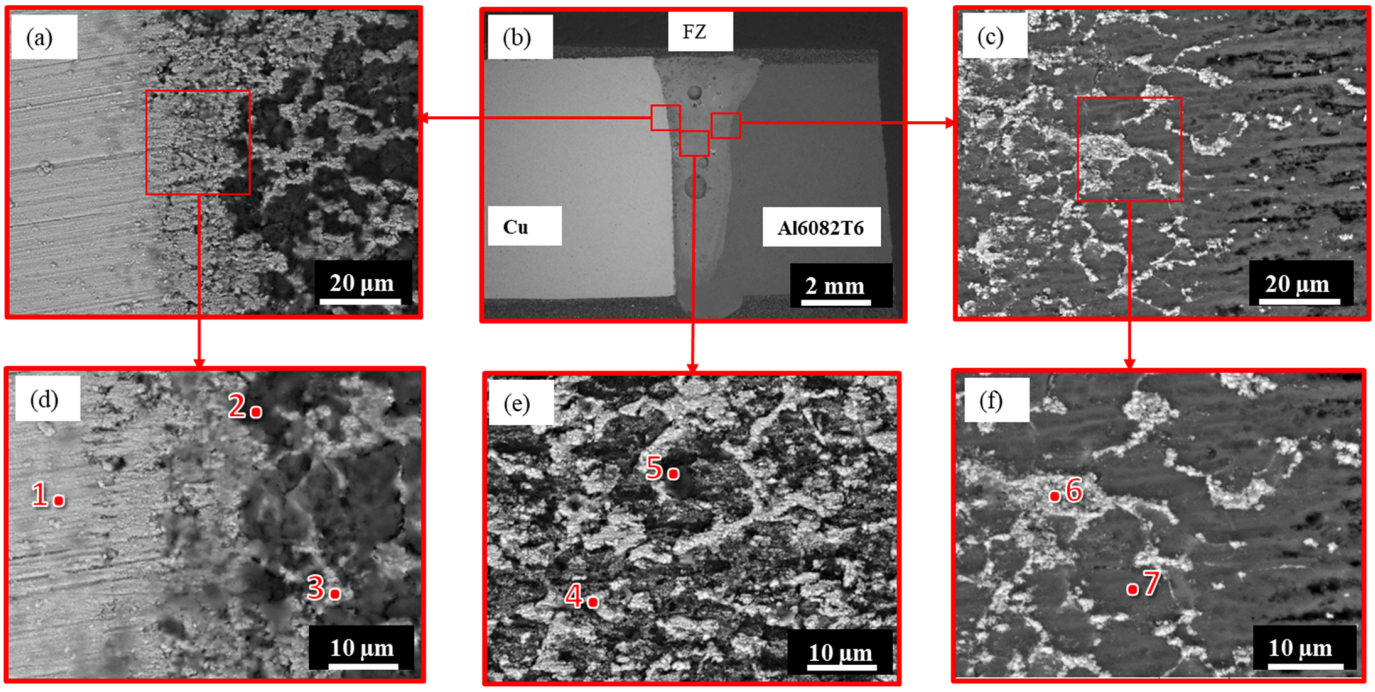


Figure 5. SEM images the cross-section of the Cu/Al6082T6 specimen with Ti filler: (**a**) interface between the copper plate and zone of fusion; (**b**) whole weld seam; (**c**) FZ-Al6082T6 interface; (**d**) image of the Cu-FZ interface; (**e**) image of the FZ; (**f**) image of the interface between the zone of fusion and the Al6082T6 alloy.

Table 2. Chemical compounds comprising the formed joint with filler.

Element	Cu, at.%	Al, at.%	Ti, at.%	Possible Phase
Point 1	89.84 ± 2.4	9.90 ± 0.2	0.26 ± 0.1	Cu
Point 2	13.14 ± 0.6	86.50 ± 2.6	0.36 ± 0.1	Al + $CuAl_2$
Point 3	36.93 ± 1.5	62.75 ± 1.9	0.32 ± 0.1	$CuAl_2$
Point 4	51.74 ± 1.9	48.13 ± 1.3	0.13 ± 0.1	CuAl
Point 5	8.54 ± 0.5	91.22 ± 3.4	0.25 ± 0.1	Al + $CuAl_2$
Point 6	26.18 ± 1.1	73.61 ± 2.2	0.21 ± 0.1	$CuAl_2$
Point 7	1.61 ± 0.1	99.02 ± 4.7	0.29 ± 0.1	Al

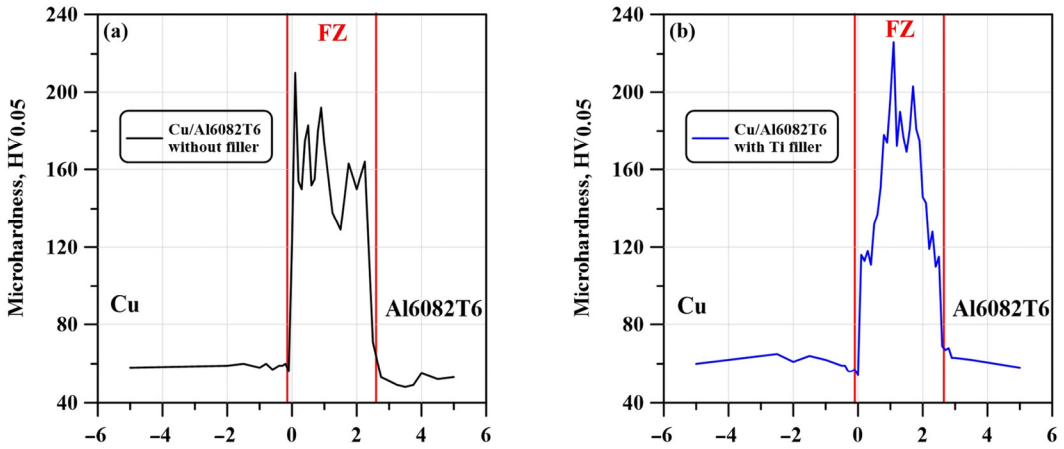


Figure 6. Microhardness at the top of samples welded (**a**) without filler and (**b**) with Ti filler.

As far as the tensile tests were concerned, the influence of the titanium filler was highly pronounced, as shown in Figure 7. The specimen without a filler showed unsatisfactory strength characteristics. It fractured after applying a tensile test force of just 400 N. For this reason, this sample's yield strength and ultimate tensile strength were not measured. The application of the titanium filler increased the strength of the formed electron beam weld significantly. The maximum tensile force reached while studying the tensile test samples had a value of 5.94 kN, which was enough to break the samples in all cases. Table 3 presents the measured mechanical properties of the samples. The presented values are averaged between the different samples. The average yield strength of the Cu/Al6082T6 welded sample with a Ti filler was 43 MPa, and the average ultimate tensile strength was 61 MPa. For comparison, the mechanical properties of the raw materials were investigated, as well. The results showed a yield strength of the pure copper plate of 267 MPa and a yield strength of the Al6082T6 alloy plate of about 217 MPa. The ultimate tensile strength of those materials had values of 275 MPa for copper and 353 MPa for the aluminum alloy plate. Copper has an elongation of about 16.8%, whereas aluminum alloy has an elongation of about 17.5%. The highest force applied to the samples prepared from the untreated plates before a fracture occurred was 21.77 kN in the case of copper and 34.69 kN in the case of Al6082T6. Low elongation of the welded samples in the present research was observed, with the average value being just 0.8%, indicating that a brittle joint was formed with low ductility. High brittleness, high hardness, and poor tensile properties are also reported by the authors of [29], who have studied Cu and Al joints formed using electron beam welding using different technological conditions. They also reported that the root cause of the poor tensile strength is the formation of IMCs in the structure of the weld seam and that during the experiments the fractures occur along the path of the IMCs [29]. The macroscopic SEM image of the sample prepared with a Ti filler shows the presence of some micro-sized pores. Their presence during the welding of Cu and Al using a high-energy electron beam seems to be typical [41]. Furthermore, the authors of [42] have studied the mechanisms of the formation of pores in the weld seams formed during the electron beam welding process.

They reported that the formation of a porous structure during electron beam welding is typical for this kind of process. Furthermore, it is known that aluminum is a material that is highly susceptible to oxidation, which could also be the cause of the present defects. Preheating of the welding plates was also performed, but at a low enough temperature so that the formation of oxide layers atop the copper plates is unlikely; however, it is known that heating aluminum samples leads to an increased solubility of H_2 in its structure [43]. This is a well-known problem when standard gas metal arc welding (GMAW) is concerned, as well [44]. At the current moment, it is not possible to tell what the composition of the gases inside the gas cavities is; however, in all cases, their presence definitely has had a negative influence on the tensile properties of the weld seams.

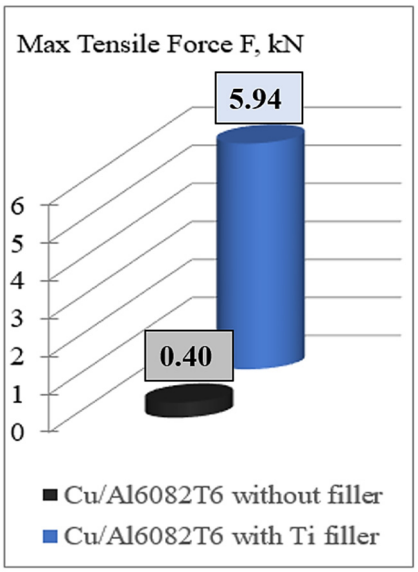


Figure 7. Break force F_b of the Cu/Al6082T6 samples without a filler and with a filler.

Table 3. Results from the tensile tests of the Cu and Al6082T6 plates and the Cu/Al6082T6 joint formed with a Ti filler.

Sample	Yield Strength, MPa	Ultimate Tensile Strength, MPa	Elongation, %	Break Force, kN
Cu	267	275	16.8	21.77
Al6082T6	217	353	17.5	34.69
Cu/Al6082T6 + Ti	43	61	0.8	5.94

4. Discussion

Copper and aluminum have the same crystal structure—a face-centered cubic crystal lattice (fcc). Titanium possesses a hexagonal close-packed crystal lattice (hcp). In addition, titanium is characterized by much lower thermal conductivity than aluminum (approximately 10 times) and copper (approximately 20 times). The volumetric thermal expansion coefficient of titanium is also about twice as low as that of aluminum and copper. These differences in the thermophysical properties of the base materials and the filler material determine the effect of the application of the Ti filler in the EBW of Cu and Al. Considering the offset toward the aluminum plate and the much lower melting temperature of aluminum compared to copper and titanium, most of the material forming the melt pool consists of aluminum. Due to the lower thermal conductivity of titanium and the very high temperature required to melt it, it is possible that most of the thermal energy generated during the contact between the electron beam and the aluminum plate was absorbed by the Ti filler. This helped the last to melt, and since less thermal energy was carried to the copper plate, less copper melted compared to the no-filler sample, limiting the formation of intermetallics at least a little bit. Furthermore, since some of the thermal energy was

absorbed by the Ti filler, this had an effect on the cooling process. A slightly finer grain structure and IMC structure were observed in the fusion zone of the Ti filler sample, which is most feasibly correlated to the change in the cooling process. Since Ti absorbed some of the thermal energy, this accelerated the cooling process and slightly refined the structure. Of course, this effect was limited due to the thin nature of the applied filler coating.

After the structural studies carried out, namely, XRD analysis, SEM, and EDX analysis, it was found that the structure of the weld seam of the Cu/Al6082T6 joint welded with Ti filler contains an aluminum solid solution, titanium, and Cu_xAl_x intermetallic compounds. According to the phase diagram of the binary system Cu–Al [45], five stable intermetallic phases can be formed in it—θ-$CuAl_2$, η-CuAl, ζ-Cu_4Al_3, δ-Cu_3Al_2, and γ-Cu_9Al_4. It is considered that the $CuAl_2$ phase forms first because it has the lowest activation energy. The crystal structure of $CuAl_2$ is body-centered tetragonal (bct). According to [45], the θ-$CuAl_2$ phase can be formed in two ways, depending on the percentage content of copper in the melt. With a larger amount of copper, about 33 at.%, the peritectic reaction L + η ↔ θ takes place. Initially, at a temperature of 624 °C, the η phase is formed from the melt, and subsequently, at a temperature of 591 °C, the θ phase is formed. In this work, it is presumed that this is the way that the intermetallic phase was formed in the sample without filler [24,46]. At a lower atomic percentage of copper in the melt, about 17%, the $CuAl_2$ phase can be formed directly from the melt by the eutectoid reaction L ↔ (Al) + θ, and at a temperature below 542.8 °C, this phase solidifies [45,47]. According to the authors of [46], this is exactly how a layer of $CuAl_2$ was formed in an aluminum-rich zone in the fusion zone during Cu–Al laser welding. The authors of [48] studied the influence of a titanium interlayer film applied between copper and aluminum and also experimentally reached the conclusion that titanium suppresses the diffusion processes between copper and aluminum. It is important to note that the diffusion processes in that work regard the transfer of copper and aluminum atoms during the deposition process, which occurs while the aluminum film is in a solid state. It is used to reduce the formation of intermetallics, and in some instances, it can prevent galvanic corrosion when the Cu–Al interface is subjected to corrosive environments [48]. In the present work, the phases that were detected were the $CuAl_2$ and the CuAl phases, but it is highly possible that other IMCs are present in the weld seam, just with low enough concentrations that they were not detected by either the XRD analysis or by the EDX analysis.

Apart from reducing the amount of molten copper, titanium has another function. The titanium atoms act as centers of crystallization and thus refine the structure of the weld. Since titanium has a higher melting point, its atoms solidify first and grains of α-Al and θ-$CuAl_2$ begin to grow around them. They hinder the grain boundary migration and inhibit the growth of grains. In this way, a finer structure is obtained. The authors of [49] proved that the addition of Tibor™ containing titanium and boron to the molten pool in laser welding of AA5083 aluminum alloy resulted in a finer structure of the weld. According to them, this additive had a more significant role in reducing the grain size in a higher cooling rate process. It is known that EBW is precisely a process characterized by high cooling rates.

The fine structure affects the mechanical properties of the compound. The finer the structure, the higher the tensile strength [50]. Our results fully agree with this statement. The application of titanium filler led to an increase in the maximal tensile force by more than an order of magnitude. Other authors also report an increase in the maximal tensile force of a copper–aluminum joint after filler application. For example, a maximal tensile force of 800 N was achieved in the laser micro-welding of Cu and aluminum with the use of silver foil versus 400 N without filler [51].

The structure of the weld and the presence of IMCs are related to the hardness. The hardness increases when a finer structure and intermetallic compounds are formed. The distribution of the measured microhardness in our experiments shows the distribution of the intermetallic phases. In the sample without filler, they are more concentrated around the interface between the fusion zone and the copper plate. While in the sample with

Ti filler, the intermetallic compounds are concentrated mainly in the middle of the weld. The slightly finer structure in this sample is evidenced by the higher measured maximum hardness value compared to the sample without filler.

5. Conclusions

In the present work, Cu and Al6082T6 plates were welded with electron beam technology by applying a Ti filler in the contact space between them. The filler was in the form of a thin layer deposited on the weld surface of each of the two plates. Applying the titanium filler on the contact surfaces between the plates had multiple effects on the welding process, such as the following:

1. The Ti layer absorbs thermal energy in order to successfully melt and be integrated into the structure of the weld seam;
2. The absorption of thermal energy by the Ti filler limited its' distribution to the copper plate, limiting the volume of the molten copper particles;
3. By absorbing some of the thermal energy of the process, the Ti filler accelerated the cooling process, resulting in a slight refinement of the particles of the weld seam;
4. The slightly finer structure and the reduced amount of brittle IMCs led to an increase in the strength of the joint. This increased the microhardness value to 235 $HV_{0.05}$. The tensile properties were also improved compared to samples prepared without a filler. The highest breaking force achieved was 5.94 kN, with an ultimate tensile strength of 61 MPa.

This work suggests that using Ti as a filler material is highly feasible when attempting to weld copper and aluminum alloys using an electron beam approach.

Author Contributions: Conceptualization, D.K., G.K. and A.A.; methodology, D.K., A.A., S.V., V.D., G.K., B.S. and M.O.; formal analysis, D.K., A.A., S.V., V.D., G.K., B.S. and M.O.; investigation, D.K., A.A., S.V., V.D., G.K., B.S. and M.O.; writing—original draft preparation, D.K. and G.K.; writing—review and editing, D.K., G.K. and S.V.; visualization, D.K. and M.O.; project administration, D.K. and A.A. All authors have read and agreed to the published version of the manuscript.

Funding: This work was supported by the Bulgarian National Scientific Fund under Grant KP-06-N47/6.

Data Availability Statement: Data are contained within the article.

Acknowledgments: Electron beam welding experiments, XRD analyses, and mechanical tests were performed thanks to the research equipment of the "Centre of competence"—BG05M2OP001–1.002–0023–C01 and "Intelligent Mechatronics, Eco- and Energy-saving Systems and Technologies" (IMEEST).

Conflicts of Interest: The authors declare no conflicts of interest.

References

1. Yang, Y.; Luo, Z.; Zhang, Y.; Su, J. Dissimilar welding of aluminum to steel: A review. *J. Manuf. Process.* **2024**, *110*, 376–397. [CrossRef]
2. Zhang, H.; Ding, H.; Li, X.; Cao, Q. A new method of magnetic pulse welding of dissimilar metal plates using a uniform pressure electromagnetic actuator based on pre-deformation. *Sci. Rep.* **2024**, *14*, 17226. [CrossRef] [PubMed]
3. Gong, Z.; Zhang, T.; Chen, Y.; Lu, J.; Ding, X.; Zhang, S.; Lan, M.; Shen, Y.; Wang, S. Effect of laser shock peening on stress corrosion cracking of TC4/2A14 dissimilar metal friction stir welding joints. *J. Mater. Res. Technol.* **2024**, *30*, 1716–1725. [CrossRef]
4. Kuryntsev, S. A Review: Laser Welding of Dissimilar Materials (Al/Fe, Al/Ti, Al/Cu)—Methods and Techniques, Microstructure and Properties. *Materials* **2022**, *15*, 122. [CrossRef]
5. Węglowski, M.S.; Błacha, S.; Phillips, A. Electron beam welding–Techniques and trends–Review. *Vacuum* **2016**, *130*, 72–92. [CrossRef]
6. Li, S.; Yue, X.; Li, Q.; Peng, H.; Dong, B.; Liu, T.; Yang, H.; Fan, J.; Shu, S.; Qiu, F.; et al. Development and applications of aluminum alloys for aerospace industry. *J. Mater. Res. Technol.* **2023**, *27*, 944–983. [CrossRef]
7. Yan, S.; Li, Z.; Song, L.; Zhang, Y.; Wei, S. Research and development status of laser micro-welding of aluminum-copper dissimilar metals: A review. *Opt. Lasers Eng.* **2023**, *161*, 107312. [CrossRef]

8. Huang, W.; Cai, W.; Rinker, T.; Bracey, J.; Tan, W. Effects of laser oscillation on metal mixing, microstructure, and mechanical property of Aluminum-Copper welds. *Int. J. Mach. Tools Manuf.* **2023**, *188*, 104020. [CrossRef]
9. Zhou, M.; Geng, Y.; Zhang, Y.; Ban, Y.; Li, X.; Jia, Y.; Liang, S.; Tian, B.; Liu, Y.; Volinsky, A. Enhanced mechanical properties and high electrical conductivity of copper alloy via dual-nanoprecipitation. *Mater. Charact.* **2023**, *195*, 112494. [CrossRef]
10. Ahmed, M.; Seleman, M.; Fydrych, D.; Cam, G. Friction Stir Welding of Aluminum in the Aerospace Industry: The Current Progress and State-of-the-Art Review. *Materials* **2023**, *16*, 2971. [CrossRef]
11. Kah, P.; Vimalraj, C.; Martikainen, J.; Suoranta, R. Factors influencing Al-Cu weld properties by intermetallic compound formation. *Int. J. Mech. Mater. Eng.* **2015**, *10*, 1–13. [CrossRef]
12. Sahin, M. Joining of aluminium and copper materials with friction welding. *Int. J. Adv. Manuf. Tech.* **2009**, *49*, 527–534. [CrossRef]
13. Cheepu, M.; Susila, P. Growth rate of intermetallics in aluminum to copper dissimilar welding. *Trans. Indian Inst. Met.* **2020**, *73*, 1509–1514. [CrossRef]
14. Abbasi, M.; Taheri, A.K.; Salehi, M.T. Growth rate of intermetallic compounds in Al/Cu bimetal produced by cold roll welding process. *J. Alloys Comp.* **2001**, *319*, 233–241. [CrossRef]
15. Wang, X.; Chen, X.; Yuan, X. Influence of filler alloy on microstructure and properties of induction brazed Al/Cu joints. *Mater. Res.* **2022**, *25*, e20210610. [CrossRef]
16. Sun, Y.; Gong, W.; Feng, J.; Lu, G.; Zhu, R.; Li, Y. A review of the friction stir welding of dissimilar materials between aluminum alloys and copper. *Metals* **2022**, *12*, 675. [CrossRef]
17. Khodir, S.A.; Ahmed, M.M.Z.; Ahmed, E.; Mohamed, S.M.; Abdel-Aleem, H. Effect of intermetallic compound phases on the mechanical properties of the dissimilar Al/Cu friction stir welded joints. *J. Mater. Eng. Perform.* **2016**, *25*, 4637–4648. [CrossRef]
18. Ouyang, J.; Yarrapareddy, E.; Kovacevic, R. Microstructural evolution in the friction stir welded 6061 aluminum alloy (T6-temper condition) to copper. *J. Mater. Process. Technol.* **2006**, *172*, 110–122. [CrossRef]
19. Galvao, I.; Loureiro, A.; Rodrigues, D.M. Critical Review on Friction Stir Welding of Aluminium to Copper. *Sci. Technol. Weld. Join.* **2016**, *21*, 523–546. [CrossRef]
20. Shin, H.; de Leon, M. Mechanical performance and electrical resistance of ultrasonic welded multiple Cu-Al layers. *J. Mater. Process. Technol.* **2017**, *241*, 141–153. [CrossRef]
21. Mathers, G. *The Welding of Aluminum and Its Alloys*; Online Book; Woodhead Publishing Ltd.: Sawston, UK, 2002; Volume 1, Chapter 3; p. 35.
22. Bunaziv, I.; Akselsen, O.M.; Ren, X.; Nyhus, B.; Eriksson, M.; Gulbrandsen-Dahl, S. A review on laser-assisted joining of aluminium alloys to other metals. *Metals* **2021**, *11*, 1680. [CrossRef]
23. Ma, B.; Gao, X.; Huang, Y.; Zhang, Y.; Huang, Y. Effect of different pulse shapes on the laser welding of aluminum and copper. *Optics Laser Technol.* **2024**, *171*, 110312. [CrossRef]
24. Kaisheva, D.; Anchev, A.; Dunchev, V.; Kotlarski, G.; Stoyanov, B.; Ormanova, M.; Valkov, S. Electron-BeamWelding Cu and Al6082T6 Aluminum Alloys with Circular Beam Oscillations. *Crystals* **2022**, *12*, 1757. [CrossRef]
25. Kaisheva, D.; Dunchev, V.; Kotlarski, G.; Stoyanov, B.; Ormanova, M.; Todorov, V.; Atanasova, M.; Valkov, S. Structure and Mechanical Properties of Cu/Al6082t6 Joints Produced by Welding with Scanning Electron Beam. *J. Tech. Univ. Gabrovo* **2023**, *66*, 46–49. [CrossRef]
26. Zhang, H.; Shi, Y.; Gu, Y.; Li, C. Effect of different filler wires on mechanical property and conductivity of aluminum-copper joints. *Materials* **2020**, *13*, 3648. [CrossRef]
27. Esser, G.; Mys, I.; Schmidt, M.H. Laser micro welding of copper and aluminium using filler materials. *Proc. SPIE* **2004**, *5662*, 337–342.
28. Feng, J.I.; Xue, S.B.; Lou, J.Y.; Lou, Y.B.; Wang, S.Q. Microstructure and properties of Cu/Al joints brazed with Zn–Al filler metals. *Trans. Nonferrous Met. Soc. China* **2012**, *22*, 281–287.
29. Otten, C.; Reisgen, U.; Schmachtenberg, M. Electron beam welding of aluminum to copper: Mechanical properties and their relation to microstructure. *Weld World* **2016**, *60*, 21–31. [CrossRef]
30. *ISO 6507-1:2018*; Metallic Materials–Vickers Harndess Test-Part 1: Test Method. ISO: Geneva, Switzerland, 2018.
31. *ISO 6892-1:2009*; Metallic Materials-Tensile Testing-Part 1; Method of Test at Room Temperature. ISO: Geneva, Switzerland, 2009.
32. Kotlarski, G.; Kaisheva, D.; Ormanova, M.; Stoyanov, B.; Dunchev, V.; Anchev, A.; Valkov, S. Improved Joint Formation and Ductility during Electron-Beam Welding of Ti6Al4V and Al6082-T6 Dissimilar Alloys. *Crystals* **2024**, *14*, 373. [CrossRef]
33. Rosa, F.; Romero, J.; Miranda, J.; Torres, A.; Rosas, G. Phase transformation of the $CuAl_2$ intermetallic alloy during high-energy ball-milling. *Intermetallics* **2015**, *61*, 51–55. [CrossRef]
34. Cai, Z.; Ai, B.; Cao, R.; Lin, Q.; Chen, J. Microstructure and properties of aluminum AA6061-T6 to copper (Cu)-T2 joints by cold metal transfer joining technology. *J. Mater. Res.* **2016**, *31*, 2876–2887. [CrossRef]
35. Fu, Y.; Zhang, Y.; Jie, J.; Svynarenko, K.; Liang, C.; Li, T. Interfacial phase formation of Al-Cu bimetal by solid-liquid casting method. *China Foundry* **2017**, *14*, 194–198. [CrossRef]
36. Kartal, F.; Yerlilkaya, Z.; Gokkaya, H. Effects of machining parameters on surface roughness and macro surface characteristics when the machining of Al-6082 T6 allot using AWJT. *Measurement* **2017**, *95*, 216–222. [CrossRef]
37. Lim, Y.; Chaudhri, M. The influence of grain size on the indentation hardness of high-purity copper and aluminum. *Philos. Mag. A* **2002**, *82*, 2071–2080. [CrossRef]

38. Han, Y.; Ben, L.; Yao, J.; Wu, C. Microstructural characterization of Cu/Al composites and effect of cooling rate at the Cu/Al interfacial region. *Int. J. Min. Met. Mater.* **2015**, *22*, 94–101. [CrossRef]
39. Das, D.; Pratihar, D.; Roy, G. Cooling rate predictions and its correlation with grain characteristics during electron beam welding of stainless steel. *Int. J. Adv. Manuf. Tech.* **2018**, *97*, 2241–2254. [CrossRef]
40. Woelke, P.; Hiriyur, B.; Nahshon, K.; Jutchinson, J. A practical approach to modelling aluminum weld fracture for structural applications. *Eng. Fract. Mech.* **2017**, *175*, 72–85. [CrossRef]
41. Mathivanan, K.; Plapper, P. Laser welding of dissimilar copper and aluminum sheets by shaping the laser pulses. *Proc. Manuf.* **2019**, *36*, 154–162. [CrossRef]
42. Huang, J.; Turner, R.; Gebelin, J.; Warnken, N.; Strangwood, M.; Reed, R. The Effect of Hydrogen on Porosity Formation during Electron Beam Welding of Titanium Alloys. In Proceedings of the 8th International Trends in Welding Research, Pine Mountain, GA, USA, 1–6 June 2008.
43. Anyalebechi, P. Hydrogen Solubility in Liquid and Solid Pure Aluminum—Critical review of Measurement Methodologies and Reported Values. *Mater. Sci. Appl.* **2022**, *13*, 158–212. [CrossRef]
44. Kotalrski, G.; Ormanova, M.; Nikitin, A.; Morozova, I.; Ossenbrink, R.; Michailov, V.; Doynov, N.; Valkov, S. Structure Formation and Mechanical Properties of Wire Arc Additively Manufactured Al4043 (AlSi5) Components. *Metals* **2024**, *14*, 183. [CrossRef]
45. Massalski, T.B.; Okamoto, H.; Subramanian, P.; Kacprzak, L.; Scott, W.W. *Binary Alloy Phase Diagrams*, 1st ed.; American Society for Metals: Metals Park, OH, USA, 1986; pp. 103–108.
46. Zobac, O.; Kroupa, A.; Zemanova, A.; Richter, K.W. Experimental description of the Al-Cu binary phase diagram. *Metall. Mater. Trans. A* **2019**, *50*, 3805–3815. [CrossRef]
47. Zuo, D.; Hu, S.; Shen, J.; Xue, Z. Intermediate layer characterization and fracture behavior of laser-welded copper/aluminum metal joints. *Mater. Des.* **2014**, *58*, 357–362. [CrossRef]
48. Yue, A.N.; Peng, K.; Zhou, L.P.; Zhu, J.J.; Li, D.Y. Influence of Ti Layer on the Structure and Properties of Al/Cu Thin Film. *Adv. Mater. Res.* **2013**, *750*, 1879–1882. [CrossRef]
49. Tang, Z.; Seefeld, T.; Vollertsen, F. Grain refinement by laser welding of AA 5083 with addition of Ti/B. *Phys. Proc.* **2011**, *12*, 123–133. [CrossRef]
50. Norouzian, M.; Elahi, M.A.; Plapper, P. A review: Suppression of the solidification cracks in the laser welding process by controlling the grain structure and chemical compositions. *J. Adv. Join. Process.* **2023**, *7*, 100139. [CrossRef]
51. Mys, I.; Schmidt, M. Laser micro welding of copper and aluminum. *Proc. SPIE* **2006**, *6107*, 28–33.

Disclaimer/Publisher's Note: The statements, opinions and data contained in all publications are solely those of the individual author(s) and contributor(s) and not of MDPI and/or the editor(s). MDPI and/or the editor(s) disclaim responsibility for any injury to people or property resulting from any ideas, methods, instructions or products referred to in the content.